Advanced Fluid Mechanics Course

Mathematical Engineering

A.A. 2020/2021

Final Project

Marangon Gaia - NM: 1242310

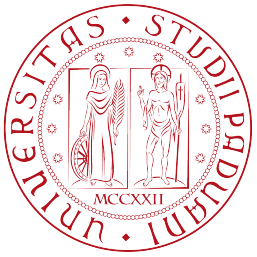

Abstract The aim of this project is to illustrate some examples of motion of irrotational fluids, reproducing the work done by Colombini M. in [2] by using the concept of complex potential. We give a general overview of the topic and we apply the main tools to derive the flow and the velocity field in some basic cases: the uniform flow, sources and sinks, the irrotational vortex, the doublet and the dipole. Then we focus on the circular cylinder with circulation, deriving its flow, velocity field, streaklines, pressure and forces on the surface. Finally, starting from the circular cylinder, we apply the Joukowski transform to derive the same quantities in the case of the Joukowski airfoil.

Contents

1 Irrotational fluids and complex potential

In this paper we treat some examples of irrotational fluids, that are fluids with no vorticity. This particular feature implies that all viscous and dissipative effects are excluded from our study, so all phenomena related to them will not appear in our simulations. This class of fluids, however, is very useful for approximating the motion of a fluid in the so called outer region, that includes all the space surrounding the bodies except for their immediate neighborhood, called inner region, where all dissipative effects take place. This is especially true when no detachment of the boundary layer is present, but we can derive some useful hints from the irrotational model even in case of detachment, if we keep away from the separation point.

Together with irrotationality, we add some more hypothesis on our fluid. We assume it to be inviscid (i.e. with no viscosity), incompressible (divergence free) and barotropic (its density depends only on pressure). With these assumptions, if we work in a non-rotating frame and with conservative body forces, we are guaranteed (by the circulation theorem) that irrotationality is preserved during the motion.

Irrotational:	$\vec{\nabla} \times \vec{u} = 0$	Inviscid:	$\nu = 0$
Incompressible:	$\vec{\nabla} \cdot \vec{u} = 0$	Barotropic:	$\rho = \rho(p)$

Moreover, some of these assumptions allow to define two special functions, the stream function and the velocity potential, which will be the basis of our procedure in simulating the flows. In particular, the incompressible continuity equation ($\partial_x u + \partial_y v = 0$, where $\vec{u} = (u, v)$ is the velocity) guarantees the existence of the stream function ψ, defined (in cartesian or in polar coordinates) as:

$$\begin{cases} u = +\partial_y \psi \\ v = -\partial_x \psi \end{cases} \qquad \text{or} \qquad \begin{cases} u_r = \frac{1}{r}\partial_\theta \psi \\ u_\theta = -\partial_r \, \psi \end{cases}$$

while the irrotationality condition ($\partial_x v - \partial_y u = 0$) guarantees the existence of the velocity potential ϕ, defined as:

$$\begin{cases} u = \partial_x \phi \\ v = \partial_y \phi \end{cases} \qquad \text{or} \qquad \begin{cases} u_r = \partial_r \, \phi \\ u_\theta = \frac{1}{r}\partial_\theta \phi \end{cases}$$

By combining these definitions we get that if the fluid is both incompressible and irrotational, then the so called Cauchy-Riemann conditions hold true:

$$\begin{cases} \partial_x \phi = +\partial_y \psi \\ \partial_y \phi = -\partial_x \psi \end{cases}$$

so that we can get immediately one of the functions ϕ, ψ once we know the other one. These conditions also imply that the equipotential lines ($\phi = \text{const}$) and the streamlines ($\psi = \text{const}$) are always orthogonal, except in the stagnation points ($u = 0$, $v = 0$). In fact:

$$\nabla\phi \cdot \nabla\psi \; = \; \partial_x \phi \, \partial_x \psi + \partial_y \phi \, \partial_y \psi \; \overset{C-R}{=} \; 0$$

which, by recalling that $\nabla\phi$ and $\nabla\psi$ are the vectors normal to the two families of curves, proves what we just stated.
Moreover, by cross differentiating the Cauchy-Riemann conditions, we get that both the stream function and the velocity potential solve the Laplace equation: $\nabla^2\phi = 0$, $\nabla^2\psi = 0$. They are therefore harmonic functions.

We recall that, for physical reasons, we need to impose two types of boundary conditions for ϕ and ψ. On solid surfaces, we have no penetration, i.e. the velocity component of the fluid which is normal to the surface must equal the corresponding velocity component of the moving surface. For a stationary body, and by denoting with s the direction along the surface and with n its normal, we get:

$$\partial_n \, \phi = 0 \qquad\qquad \partial_s \, \psi = 0 \qquad\qquad \text{on stationary surface}$$

Besides, as a condition at infinity we usually assume a uniform motion along x with constant speed U. Therefore we have:

$$\partial_x \, \phi = U \qquad\qquad \partial_y \, \psi = U \qquad\qquad \text{at infinity}$$

Finally, we recall that the solutions of the Laplace equation are subjected to linearity. This means that the superposition of harmonic functions is still an harmonic function, with a new set of boundary conditions resulting from the combination of the original boundary conditions. This property is fundamental in our study, since it allows us to describe more complicated problems as the superposition of simpler cases, whose flow is computed in an easy way.

With this setting, we can summarize the general procedure to solve this kind problems:

- find ϕ or ψ by solving the Laplace equation;
- find $\vec{u} = (u,\, v)$ by differentiating ϕ or ψ;
- find the pressure p by applying the Bernoulli theorem: $p_A + \rho\frac{u_A^2+v_A^2}{2} = p_B + \rho\frac{u_B^2+v_B^2}{2}$ at any two points A, B.

In our case, the first point of this procedure is treated in a different way. We make use of a special quantity called complex potential, defined as:

$$w = \phi + i\,\psi$$

which is a complex function whose real part coincides with the velocity potential and whose imaginary part coincides with the stream function. This complex function has two relevant properties, coming from the fact that the stream function and the velocity potential satisfy the Cauchy-Riemann conditions. First of all, since ϕ and ψ are functions of (x, y), also w should be in principle a function of (x, y). However, due to Cauchy-Riemann conditions, it can be shown that the dependence of w on (x, y) is in fact a dependence on a special combination of the two:

$$w(x, y) \;=\; w(x + i\,y) \;=\; w(z)$$

Besides, the derivative $\frac{dw}{dz}$ is unique, meaning that it does not depend on the direction of δz as δz tends to zero. It represents the velocity components:

$$\frac{dw}{dz} = u - i\,v$$

These properties are in fact a characterization: it can be shown that *any* function of the form $w(z) = \phi(x, y) + i\,\psi(x, y)$ whose derivative $\frac{dw}{dz}$ is unique in the above sense, represents the complex potential of some irrotational flow, with ϕ, ψ satisfying Cauchy-Riemann conditions and solving the Laplace equation in the (x, y) plane.

This fact is a fundamental basis in our study: in the following section we present some elementary examples of irrotational flow and the starting point is precisely the definition of a complex function $w(z) = w(x + i\,y)$. Once assigned this function, we interpret it as complex potential, we get the corresponding stream function and velocity potential as its imaginary and real part, and then we proceed as mentioned above to find the velocity field and possibly the pressure. At the end of the procedure, it becomes clear what is the physical situation described by the initially assigned complex potential. For further readings about this approach, see [3].

2 Elementary Flows

In this section we present a list of simple flows of irrotational fluid, starting with some elementary cases (uniform flow, sources and sinks, irrotational vortex) and then showing some basic examples of combinations (dipole, doublet). Following what is described in the previous section, we start by defining the complex potential $w(z)$, then we isolate its real and imaginary part to get the velocity potential and the stream function, and finally we compute the velocity field by taking the proper derivatives.

In each case, the results were implemented in MATLAB, yielding the plots for streamlines, equipotential lines and velocity field. Further elementary examples, treated in a theoretical way, can be found in [3].

2.1 Uniform Flow

This basic example of complex potential represents a uniform flow along the x axis of speed U. It is usually combined with other types of flow to model the behavior of the fluid far away from any bodies or surfaces. It can be derived as follows:

Complex potential:	$w = Uz$	
Real, Imaginary part:	$\phi = Ux$	$\psi = Uy$
Velocity components:	$u_x = \partial_x \phi = U$	$u_y = \partial_y \phi = 0$

The resulting functions appear as follows.

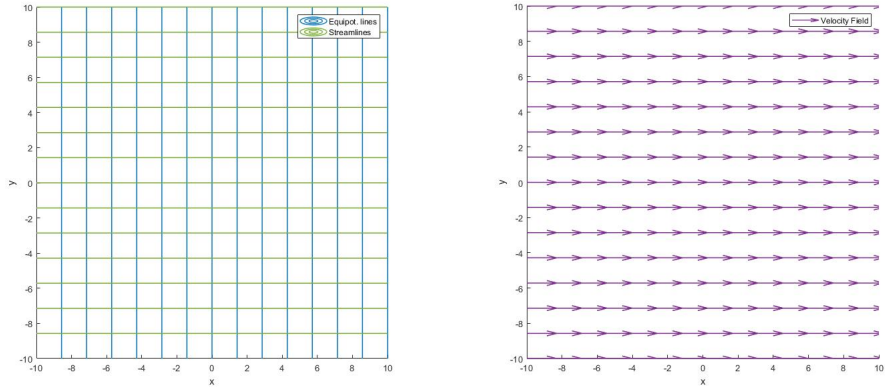

(a) Equipotential lines and Streamlines

(b) Velocity Field

Figure 1: Uniform Flow

We notice that the velocity is always tangent to the streamlines,while the equipotential lines are perpendicular to both. The resulting flow is horizontal and uniform, as mentioned above.

2.2 Sources and Sinks

This second complex potential represents a source or a sink of the flow. The main parameter m represents the volume flow rate per unit depth ($m = \int_0^{2\pi} u_r \, r \, d\theta$) and is positive for the source and negative for the sink. We derive the main quantities as usual:

Complex potential:	$w = \frac{m}{2\pi} ln(z) = \frac{m}{2\pi} ln(re^{i\theta})$	$= \frac{m}{2\pi} ln(r) + \frac{m}{2\pi} (i\theta)$
Real, Imaginary part:	$\phi = \frac{m}{2\pi} ln(r)$	$\psi = \frac{m}{2\pi} \theta$
Velocity components:	$u_r = \partial_r \phi = \frac{m}{2\pi r}$	$u_\theta = -\partial_r \psi = 0$

The corresponding plots are as follows.

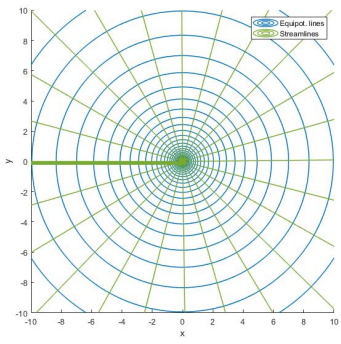

(a) Equipotential lines and Streamlines

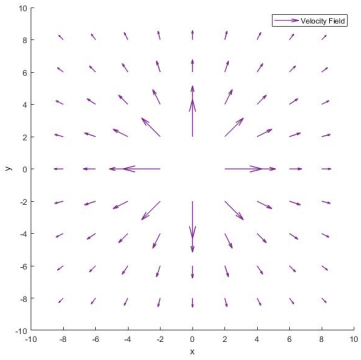

(b) Velocity Field

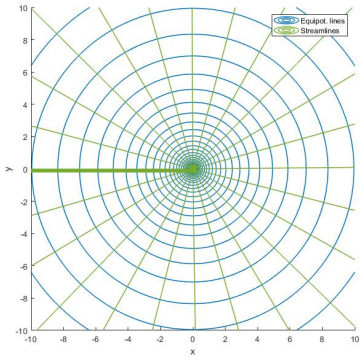

(c) Equipotential lines and Streamlines

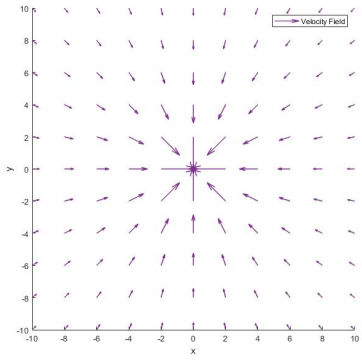

(d) Velocity Field

Figure 2: Source (above) and sink (below)

We observe that the velocity field, together with the streamlines, is directed radially, and points away from the center in the case of sources and towards the center in the case of the sink: in the former case, the fluid is therefore dispersed towards infinity, while in the latter case it accumulates in the origin. In both cases, the origin plays the role of a singular point, generating or absorbing mass. As for the equipotential lines, being orthogonal to the streamlines, they form concentric circles centered at the origin. Across them, the total mass flux is always equal to the parameter m.

Furthermore, we notice a thicker line on the left in the streamlines plot. It is due to the fact that the complex potential is a multi-valued function of space: at every point the potential is known up to a constant. This however does not prevent us from finding the velocity field: since it is computed through differentiation, its value in know uniquely at every point of the space.

2.3 Irrotational Vortex

A slight modification of the previous complex potential leads to the irrotational vortex. In this case the main paramenter is called Γ and represents the circulation of the vortex, in counterclockwise direction. The main quantities are derived as above:

Complex potential:	$w = -i\,\dfrac{\Gamma}{2\pi}\,ln(z) = -i\,\dfrac{\Gamma}{2\pi}\,ln(re^{i\theta})$	$= -\,i\,\dfrac{\Gamma}{2\pi}\,ln(r) - i\dfrac{\Gamma}{2\pi}\,(i\theta)$
Real, Imaginary part:	$\phi = \dfrac{\Gamma}{2\pi}\,\theta$	$\psi = -\dfrac{\Gamma}{2\pi}\,ln(r)$
Velocity components:	$u_r = \partial_r \phi = 0$	$u_\theta = -\partial_r \psi = \dfrac{\Gamma}{2\pi r}$

The resulting plots are as follows.

In this case the role of the streamlines and of the equipotential lines is inverted: the former are circles centered at the origin, while the latter are radial. The fluid is rotating in circles, as expected for a vortex.

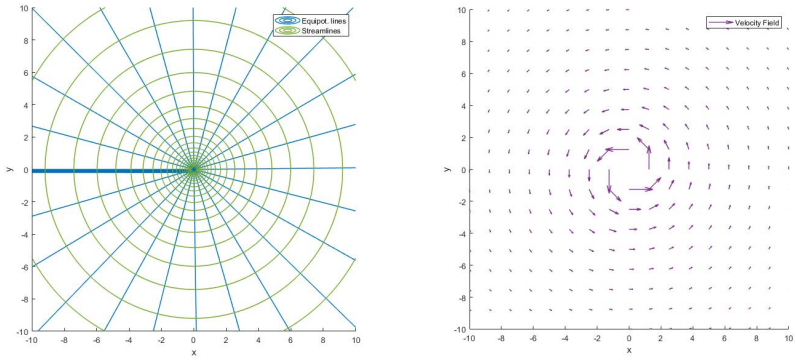

(a) Equipotential lines and Streamlines (b) Velocity Field

Figure 3: Irrotational Vortex

2.4 Dipole

In this example we show the first application of the superposition principle: we combine a source and a sink of the same strength, located at $x = -a$ and $x = a$ respectively, and we obtain a configuration known as dipole. The complex potential is defined as the sum of the complex potentials of the source and the sink, taking into account their displacement. Then the computations are carried out as usual:

Complex potential:
$$w = \frac{m}{2\pi} ln(z+a) - \frac{m}{2\pi} ln(z-a) = \frac{m}{2\pi} ln\left(\frac{z+a}{z-a}\right)$$
$$= \frac{m}{2\pi} ln\left(\frac{\sqrt{(x+a)^2+y^2}\, e^{i\, atan\frac{y}{x+a}}}{\sqrt{(x-a)^2+y^2}\, e^{i\, atan\frac{y}{x-a}}}\right)$$

Real, Imaginary part:
$$\phi = \frac{m}{2\pi} ln\left(\frac{\sqrt{(x+a)^2+y^2}}{\sqrt{(x-a)^2+y^2}}\right) \qquad \psi = \frac{m}{2\pi}\left(atan\frac{y}{x+a} - atan\frac{y}{x-a}\right)$$

Velocity components:
$$u_x = \partial_y \psi = \frac{m}{2\pi}\left(\frac{x+a}{(x+a)^2+y^2} - \frac{x-a}{(x-a)^2+y^2}\right)$$
$$u_y = -\partial_x \psi = \frac{m}{2\pi}\left(\frac{y}{(x+a)^2+y^2} - \frac{y}{(x-a)^2+y^2}\right)$$

The results are reported in the following plots.

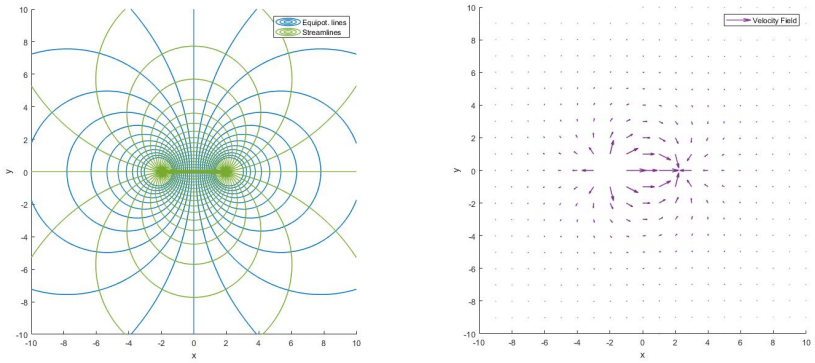

(a) Equipotential lines and Streamlines (b) Velocity Field

Figure 4: Dipole

We observe that the velocity field, together with the streamlines, forms pieces of circumferences with

increasing radius and with centers located on the y axis. According with the previous results for sources and sinks, the velocity is always pointing away from the source and towards the sink. On the other side, the equipotential lines form closed circles with increasing radius and with center on the x axis, keeping orthogonal to the streamlines at every point of the space. As in the previous examples of sources and sinks, the points $(-2, 0)$ and $(-2, 0)$ are singularities of the complex potential.

2.5 Doublet

In this last example we start from the same combination of source and sink we've already described in the dipole, but this time we let their positions collapse into a unique point, by setting: $(x = -\epsilon, y = 0)$, $(x = \epsilon, y = 0)$ with $\epsilon \to 0$.

In this case the complex potential is built starting from the one of the dipole, by expanding it in Taylor series (using $ln\left(\frac{1+x}{1-x}\right) = 2x + \frac{2}{3}x^3 + \dots$, with $x = \frac{\epsilon}{z}$) and by truncating it at the second order of approximation:

$$w = \frac{m}{2\pi} ln(z+\epsilon) - \frac{m}{2\pi} ln(z-\epsilon) = \frac{m}{2\pi} ln\left(\frac{z+\epsilon}{z-\epsilon}\right) = \frac{m}{2\pi} ln\left(\frac{1+\frac{\epsilon}{z}}{1-\frac{\epsilon}{z}}\right) \simeq \frac{m\epsilon}{\pi z} \to \frac{\mu}{z}$$

where we denoted $\mu := \lim_{\epsilon \to 0} \frac{m\epsilon}{\pi}$, assumed to be finite. With this setting, we can proceed with our usual analysis:

Complex potential:
$$w = \frac{\mu}{z} = \frac{\mu}{r} e^{-i\theta} = \frac{\mu r}{r^2}\left(cos\theta - i\, sin\theta\right) = \mu \frac{x - iy}{x^2 + y^2}$$

Real, Imaginary part:
$$\phi = \frac{\mu x}{x^2 + y^2} \qquad \psi = -\frac{\mu y}{x^2 + y^2}$$

Velocity components:
$$u_x = \partial_x \phi = \mu \frac{y^2 - x^2}{(x^2 + y^2)^2}$$
$$u_y = \partial_y \phi = -2\mu \frac{xy}{(x^2 + y^2)^2}$$

The resulting plots are as follows.

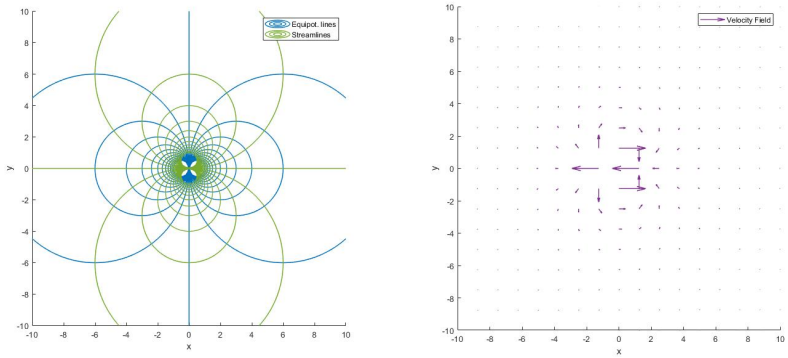

(a) Equipotential lines and Streamlines (b) Velocity Field

Figure 5: Doublet

The resulting plots are similar to the ones of the dipole, but now the source and sink coincide, yielding a unique singular point. The streamlines describe complete circles, resulting in a pattern which is analogous to the one of the equipotential lines, but rotated by ninety degrees.

As for the velocity, its strong gradient when moving away from the center causes the figure to be not so immediate to read. However we're still able to confirm that the velocity field is tangent to the streamlines at every point of the space and is going out of the singularity on the left, where the source was originally located, while it points towards the singularity on the right, in accordance with the original position of the sink.

3 Circular Cylinder

In this section we focus on a special combination of elementary cases, representing the motion of an irrotational fluid around a circular cylinder. This case is particularly meaningful since it can be used as an intermediate step to compute the flow around a special class of airfoils, the so called Joukowski airfoils, that will be treated in the next section.

As usual, we start by defining the complex potential. In this case, it results from the superposition of a uniform flow (with speed U, directed along the x axis), a doublet (with the same setting described in the previous section) and an irrotational vortex (assumed to be clockwise, i.e. with circulation $-\Gamma$, $\Gamma > 0$). We also add a new parameter a which normalizes the argument of the logarithm to make it dimensionless and which plays the role of the radius of the circular cylinder.

References about this topic can be found in [3] and [1].

3.1 Streamlines, Equipotential Lines and Velocity

With the given setting, we start our analysis by deriving the stream function, the velocity potential and the velocity field, following the usual procedure.

Complex potential: $$w = Uz + \frac{\mu}{z} + i\,\frac{\Gamma}{2\pi} ln\left(\frac{z}{a}\right) \qquad = U\left(z + \frac{a^2}{z}\right) + i\,\frac{\Gamma}{2\pi} ln\left(\frac{z}{a}\right)$$

Real, Imaginary part: $$\phi = U\left(r + \frac{a^2}{r}\right) cos\theta - \frac{\Gamma}{2\pi}\theta \qquad \psi = U\left(r - \frac{a^2}{r}\right) sin\theta + \frac{\Gamma}{2\pi} ln\left(\frac{z}{a}\right)$$

Velocity components: $$u_r = \frac{1}{r}\partial_\theta \psi = U\left(1 - \frac{a^2}{r^2}\right) cos\theta \qquad u_\theta = \frac{1}{r}\partial_\theta \phi = -U\left(1 + \frac{a^2}{r^2}\right) sin\theta - \frac{\Gamma}{2\pi r}$$

The values of the parameters are arbitrary, but we made some specific choices, in order to be already in accordance with the airfoil setting which will be treated later on. First, we choose the speed U to be negative, i.e. moving from the right to the left along the negative direction of the x axis. Then, we choose a negative value for the circulation Γ, in order to make it anticlockwise. Finally, the choice of the modulus of the circulation is based on a specific critical value, whose role will be clarified later on: $\Gamma_* = 4\pi a U$. We plot the functions of interest for $\Gamma = 0$, $\Gamma = \frac{\Gamma_*}{2}$ and $\Gamma = \Gamma_*$.

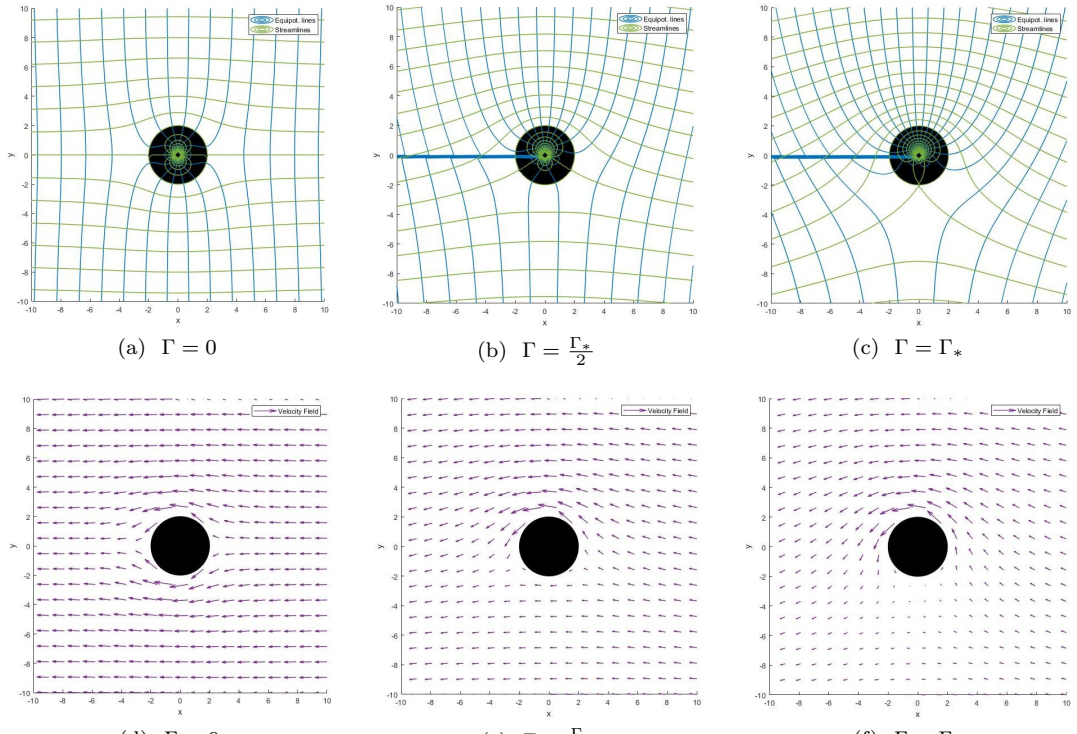

(a) $\Gamma = 0$ (b) $\Gamma = \frac{\Gamma_*}{2}$ (c) $\Gamma = \Gamma_*$

(d) $\Gamma = 0$ (e) $\Gamma = \frac{\Gamma_*}{2}$ (f) $\Gamma = \Gamma_*$

Figure 6: Streamlines and Equipotential lines (above) and Velocity (below)

We start our observation from the graphs obtained for $\Gamma = 0$. In this case all the patterns are symmetric with respect to the x axis and the velocity field moves around the cylinder with the same

speed above and below the cylinder. Two stagnation points are visible: they are located on the surface of the cylinder and they are symmetric with respect to the y axis: $(-a, 0)$ and $(a, 0)$.

As the circulation grows in modulus, the symmetry with respect to the x axis is broken: the streamlines become more dense above the cylinder, where the speed grows larger, while they are more separated below the cylinder, where the speed grows smaller. This is due to the fact that on the top the circulation is in accordance with the velocity, causing it to increase, while in the lower part the circulation moves against the velocity, reducing it. In accordance to this behavior, we note that the stagnation points are moving towards the bottom of the cylinder. They're still on the surface and they're still symmetric with respect to the y axis, but their y coordinate is lowering.

As $\Gamma = \Gamma_*$, we reach a critical situation: the two stagnation points collapse into a unique point, still lying on the surface, at position $(0, -a)$. This is the last value of the circulation for which the velocity attains the value zero on the surface. As the modulus of the circulation increases beyond this critical value, the unique stagnation point detaches from the surface, moving lower and lower along the y axis.

3.2 Streaklines

Streaklines are the sets of all positions occupied by particles which had passed through a specific point of the space at some time in the past. To give a practical idea, they can be visualized by injecting punctually some ink or other marked fluid into our main fluid, and by observing at each instant of time the pattern formed by the marked particles.

Since we're dealing with a stationary flow, the streaklines coincide with the streamlines (lines which are tangent at every point to the velocity field) and with the pathlines (trajectories of individual particles of the fluid). With this setting, the streaklines are given by the solutions of the following system, for a given arbitrary set of initial conditions (r_0, θ_0).

$$\begin{cases} \frac{dr}{dt} = u_r = +U\left(1 - \frac{a^2}{r(t)^2}\right) cos\theta(t) \\ \frac{d\theta}{dt} = u_\theta = -U\left(1 + \frac{a^2}{r(t)^2}\right) sin\theta(t) - \frac{\Gamma}{2\pi r(t)} \\ r(0) = r_0 \\ \theta(0) = \theta_0 \end{cases}$$

The system can be solved by discretizing the time domain (the index k will be used to run over the time) and by applying a finite difference scheme, for example the explicit Forward Euler. In this case the right end sides are evaluated at the current instant of time (index k) and are used to update the function of interest at the subsequent instant of time ($r(k+1)$ and $\theta(k+1)$). This iterative procedure can be expressed explicitly as:

$$\begin{cases} \frac{r(k+1)-r(k)}{\triangle t} = +U\left(1 - \frac{a^2}{r(k)^2}\right) cos\theta(k) \\ \frac{\theta(k+1)-\theta(k)}{\triangle t} = -U\left(1 + \frac{a^2}{r(k)^2}\right) sin\theta(k) - \frac{\Gamma}{2\pi r(k)} \\ r(0) = r_0 \\ \theta(0) = \theta_0 \end{cases}$$

In this way we're able to draw the streaklines for different values of the circulation (they are kept lower than before to facilitate the visualization). In this case the moving particles are divided into blocks of different colors, so that we can better appreciate the change of velocity as we move in the neighborhood of the cylinder.

Starting from the first graph, where $\Gamma = 0$, we notice that the motion of the fluid is symmetrical with respect to the x axis, as it was for streamlines and equipotential lines. However, the particles which move closer to the cylinder are slower than the ones far away from it, as we can perceive by observing the length of the colored block, which is shorter in the former case and longer in the latter. This is due to the fact that the particles tend to slow down as they get near to the stagnation points.

As the circulation increases, this difference in length becomes more visible, and symmetry is lost. Particles above the cylinder move faster than the corresponding particles below the cylinder, in accordance to the fact that the stagnation points are lowering down and are therefore slowing down the particles on the bottom. This effect becomes more and more visible as the circulation increases, resulting in a more marked deformation of the initial blocks.

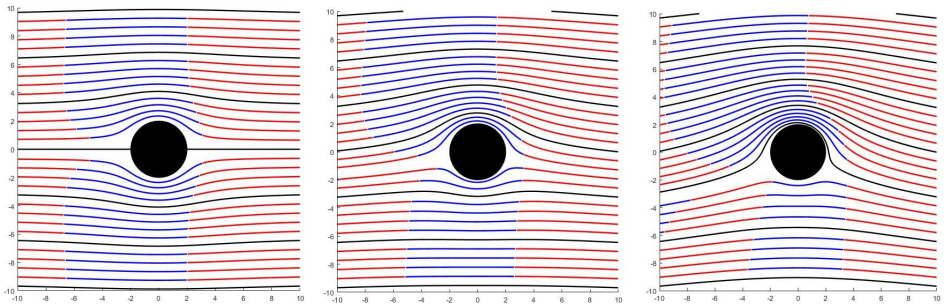

(a) $\Gamma = 0$ (b) $\Gamma = \frac{\Gamma_*}{4}$ (c) $\Gamma = \frac{\Gamma_*}{2}$

Figure 7: Streaklines

3.3 Pressure

The next step in our analysis consists in computing the pressure field around the cylinder. In order to do this, we can exploit the Bernoulli theorem, which states that a particular combination of pressure and velocity is constant all over the space. We choose a reference point located at infinity, where velocity and pressure are known ($U\hat{x}$, p_∞, i.e. the values of the unperturbed uniform flow) and we compare it with any other point of the space, where the velocity (u_r, u_θ) is known from the previous analysis and the pressure p is the value we want to compute. In our case, we choose to derive and plot a normalized version of the pressure: $\frac{p-p_\infty}{\rho U^2}$, which is dimensionless. More explicitly:

$$p_\infty + \rho\frac{U^2}{2} = p + \rho\frac{u_r^2 + u_\theta^2}{2} \qquad \Leftrightarrow \qquad \frac{p - p_\infty}{\rho U^2} = \frac{1}{2}\left(1 - \frac{u_r^2 + u_\theta^2}{U^2}\right)$$

It is also possible to rewrite the pressure as a function of the polar coordinates (r, θ), simply by substituting the expressions we have found for u_r, u_θ:

$$\frac{p - p_\infty}{\rho U^2} = \frac{1}{2}\left(- \frac{a^4}{r^4} + \frac{a^2}{r^2}\, 2cos(2\theta) - \left(\frac{\Gamma}{2\pi r U}\right)^2 - \frac{\Gamma}{\pi r U}\left(1 + \frac{a^2}{r^2}\right) sin\theta \right)$$

The results are plotted in the following, for three different values of the circulation.

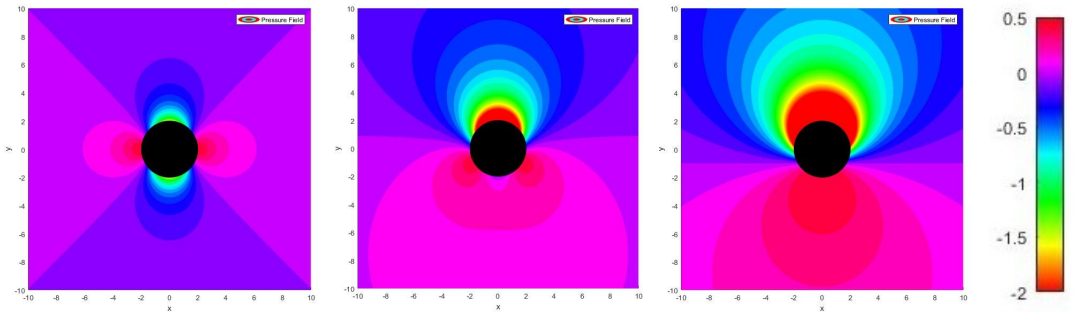

(a) $\Gamma = 0$ (b) $\Gamma = \frac{\Gamma_*}{2}$ (c) $\Gamma = \Gamma_*$

Figure 8: Pressure

In the first graph, with no circulation, we observe the same symmetry with respect to the x and y axis we've already observed in all corresponding previous graphs. The pressure is positive on the sides and attains its maximum value in correspondence of the stagnation points, where the square velocity attains its minimum; while it is negative above and below the cylinder and attains its minimum at the top and at the bottom points of the surface, where the velocity is maximum.

As the circulation increases, the behavior of the pressure follows the one of the velocity: the symmetry with respect to the x axis is broken and the maximum points for the pressure are progressively lowered, being always in coincidence with the stagnation points. The pressure increases below the cylinder and decreases above it.

When the circulation attains its critical value, the maximum points collapse into a unique point, again the stagnation point. The pressure is now positive below the cylinder and negative above it. This fact, that is more and more marked as the circulation increases, has important consequences on the forces acting on the body, as we're going to see in the following.

3.4 Forces

We're now interested in computing the elemental forces acting on the surface of the cylinder. Since we're focusing on a section of the cylinder, the forces will be expressed per unit length. With this convention we can write:

$$\vec{F} = -p\hat{n}\, ds = -p\hat{n}R\, d\theta$$

where p is the pressure, $\hat{n} = (cos\theta, sin\theta)$ is the outer unit normal and $ds = R\, d\theta$ is the elemental length arc, described as a function of the radius and of the elemental angle. In our case we focus on the normalized pressure $\frac{p-p_\infty}{\rho U^2}$ and we compute the corresponding normalized forces. This allows us to get a complete description of the problem without specifying any further parameter (p_∞, ρ).

In the following we show the results for the three usual values of the circulation.

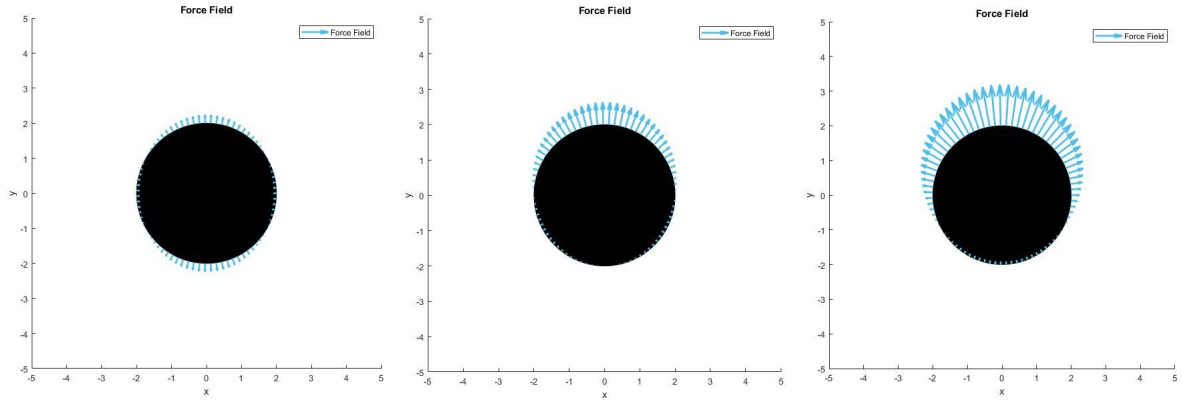

(a) $\Gamma = 0$ (b) $\Gamma = \frac{\Gamma_*}{2}$ (c) $\Gamma = \Gamma_*$

Figure 9: Forces on surface

From this graphs we can see immediately the strict relation between forces and pressure.

In the first graph, preserving the usual symmetry with respect to both axis, the forces are directed towards the interior of the cylinder at the left and at the right sides, where the pressure is positive; while they are directed towards the exterior of the cylinder at the top and at the bottom, where the pressure is negative.

In the second graph, the regions where the forces point towards the center are lowered, in correspondence with the maximum points of pressure and with the stagnation points. Together with this, the forces are reduced in intensity below the cylinder, where the pressure is progressively passing from negative to positive values; while they are increasing in intensity above the cylinder, where the pressure is becoming more and more negative.

This behavior is even more visible in the third graph, showing extremely intense forces above the cylinder and increasing forces below it, where the pressure is now attaining higher and higher positive values, causing the forces to point towards the interior of the cylinder.

To conclude, we notice that the forces are always symmetrical with respect to the y axis. This causes the total force acting on the body to be entirely directed along the y axis, with no x component. In other words, no drag force is acting on the cylinder, as expected for an inviscid fluid. On the contrary, the presence of non-zero circulation is responsible for a lift force acting along the vertical direction. It can be shown that this force depends only on the circulation Γ, on the velocity of the fluid at infinity U and on the density ρ of the fluid.

$$L = \rho U \Gamma$$

This result, known as Kutta-Joukowski Lift Theorem, holds true for all kinds of cylinder, independently on the shape of the section.

4 Joukowski Airfoil

The last part of our project is aimed at studying a special class of airfoils, the so called Joukowski airfoils. They are obtained by applying a specific geometrical transformation - the Joukowski transform - to a circular cylinder, mapping it into an airfoil-like shape. This special construction allows us to derive the flow of an irrotational fluid around the airfoil by exploiting the results we already have for the circular cylinder, mapping them into the new results with the help of the Joukowski transform.

It must be noticed, however, that not all airfoils can be obtained with this procedure. This technique is in fact quite limited, and its relevance is mainly of historical nature. For the sake of completeness, we mention the fact that other analytical techniques were developed, generalizing Joukowski strategy to a much wider range of airfoils, so that - for example - with Theodorsen's method we are able to study whatever airfoil, by defining an adapted transformation which maps it into a circle. These extended strategies, however, are considerably complicated, so we will focus only on the original method proposed by Joukowski.

4.1 Joukowski Transformation

The Joukowski transformation is defined as:

$$z = \zeta + \frac{b^2}{\zeta} \qquad \text{with: } z = x + i\,y, \quad \zeta = \xi + i\,\eta$$

It is a complex function, mapping the complex ζ-plane (with ξ real coordinate and η imaginary coordinate) into the complex z-plane (with x real coordinate and y imaginary coordinate). It has the property of being conformal, that is, it preserves angles and infinitesimal lengths, but it does not preserve finite lengths, which are therefore deformed in the arrival space (see [5] for more details about conformal mapping).

To give an idea of how the ζ-plane is mapped into the new z-plane, we can set a uniform polar grid in the former plane and observe how it is deformed in the latter:

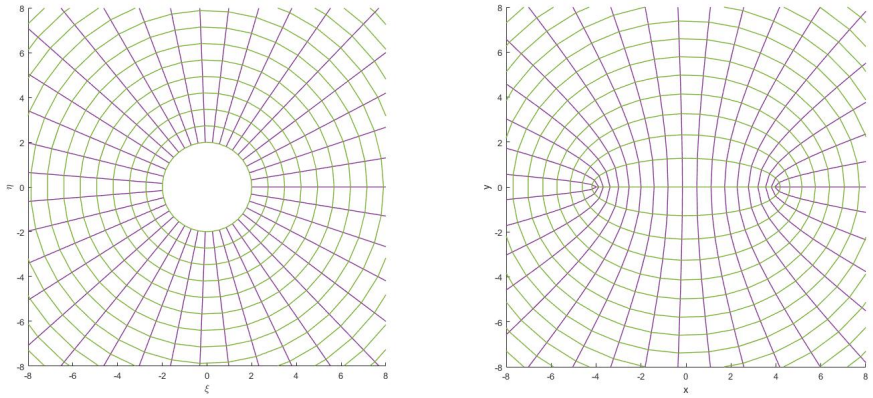

(a) ζ-plane (b) z-plane

Figure 10: Joukowski Transform

With this transformation, a circle in the ζ-plane becomes an airfoil-like shape in the z-plane. We will therefore interpret the z-plane as the (x, y) physical space where the airfoil is placed, and the ζ-plane as an ideal physical space - the (ξ, η) bidimensional space - where the circle is defined.

At this point, we can set the basis of our procedure to compute the flow around the airfoil. The fundamental idea is to use the Joukowsky transformation to write the complex potential $w_a(z)$ of the airfoil as a function of the complex potential $w_c(\zeta)$ of the circular cylinder, which is already known. This can be done through a simple composition:

$$w_a(z) = w_c(\zeta(z))$$

In this way the complex potential of the airfoil is fully described. Starting from it, we can apply the usual procedure: we derive the velocity potential and the stream function as its real and imaginary part; we compute the velocity field through differentiation; we use Bernoulli to obtain the pressure field and therefore the forces on the surface.

4.2 From Circular Cylinder to Airfoil

Before we start with the derivation of all the main functions, we want to illustrate in a more detailed way what are the features of the Joukowski airfoil in terms of shape, and how they are related to the properties of the circle we start from. Proofs of the following statements can be found in [3], while an alternative geometrical construction is treated in [4].

In the easiest case, we start from a circle centered in the origin, with radius b equal to the parameter in the Joukowski transform. In this elementary case, the circle is mapped into a straight line along the x axis, going from $x = -2b$ to $x = 2b$, showing neither thickness nor curvature.

We may now shift the center of the circle along the x axis, of a small quantity $x_c = eb$, where $e << b$. The resulting airfoil is now thicker, with a rounded leading edge and a cusped trailing edge. The profile is still symmetric with respect to the x axis, showing no curvature.

On the other side, we may shift the circle along the y axis, of a quantity $y_c = a \cdot tan\beta$, where: $a = b(e+1)$ is the length of the segment connecting the projection of the center on the x axis to the point of intersection between the circle and the positive x axis; while β is the angle formed by the center of the circle, the point of intersection between the circle and the positive x axis, and the origin of the plane. In this case, the circle is mapped into a curved line: no thickness is present, but the profile is cambered, forming an angle of 2β with the x axis.

Finally, if we combine both shifts for the center, we get the most generic Joukowski profile, endowed with both thickness and camber.

All these possible configurations are summarized in the following figures.

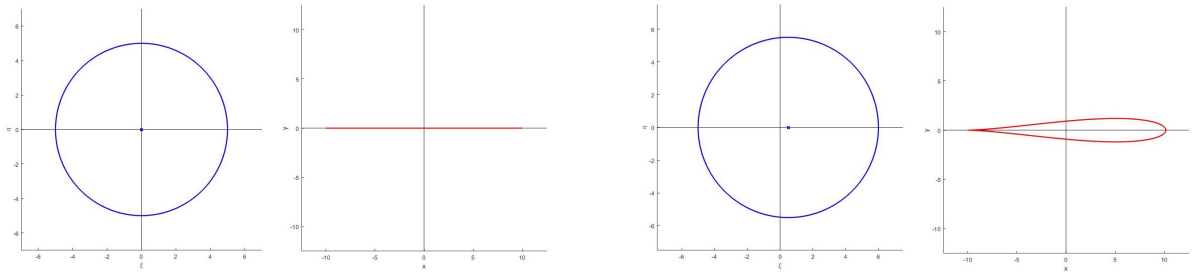

(a) Center in $(0, 0)$, ζ-plane

(b) Center in $(0, 0)$, z-plane

(c) Center in $(x_c, 0)$, ζ-plane

(d) Center in $(x_c, 0)$, z-plane

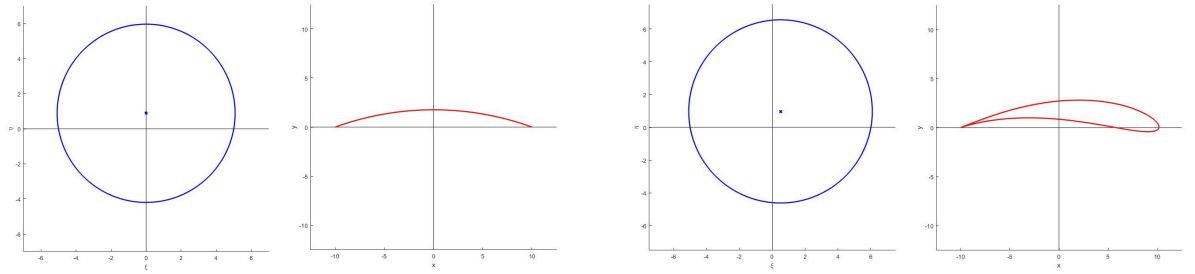

(e) Center in $(0, y_c)$, ζ-plane

(f) Center in $(0, y_c)$, z-plane

(g) Center in (x_c, y_c), ζ-plane

(h) Center in (x_c, y_c), z-plane

Figure 11: Airfoil profiles

To conclude our description, we anticipate that we will be interested in studying the last and most generic type of airfoil, assuming for it an inclination of angle α with respect to the x axis. This is called angle of attack and represents the relative inclination between the airfoil and the uniform flow coming from the right at infinite distance.

4.3 Kutta condition

To conclude the description of our initial setting, we need to make another important remark about circulation and stagnation points. This topic can be found in [4].

Up to now, we're considering a circle in the ζ-plane, with shifted center, and invested by a uniform flow coming from infinity with an angle of attack α. With this construction, a stagnation point should appear in the upper face of the airfoil, near the trailing edge. However, this would result in a very counterintuitive situation: particles moving along the lower face of the airfoil should follow the profile, make a sharp turn

around the trailing edge and then go back along the upper face, up to the stagnation point, from which they can leave the surface. This is not a good description of the real physical phenomenon.

To solve this problem, we may introduce a counterclockwise circulation around the airfoil. This would result in a downwards shift of the stagnation point, which, for a specific value of the circulation, would eventually coincide with the trailing edge. With this configuration, particles flowing in the lower face would simply leave the surface once reached the trailing edge, without turning sharply and moving backwards along the upper face. This is what we would expect from a real airfoil. This guess is known as Joukowski hypothesis or Kutta condition: they suggest that the circulation around a real airfoil naturally adjusts itself so that the stagnation point of the cylinder is mapped exactly into the trailing edge. This guess is confirmed with good approximation for well designed airfoil, so it can be adopted as the right description of the problem.

This guess has of course a physical explanation, but it needs a tool which was not considered up to now for irrotational fluids: the viscosity. Actually, when the flow has just started and the circulation is not present yet, particles moving along the lower face really try to turn around the trailing edge, but meet the opposition of viscous forces, which prevent them from moving backwards along the upper face and cause them to leave the surface in advance, forming a clockwise vortex in the neighborhood of the trailing edge. Now we know from the circulation theorem - holding true under our working hypothesis - that the total circulation along a close curve must be preserved during the motion. In our case the initial circulation was zero along any path, so if we consider a circuit enclosing both the vortex and airfoil, the total circulation along it must still be zero. The only possibility is that an anticlockwise circulation is established around the airfoil, balancing at every moment the one of the vortex.

To conclude, and therefore be able to proceed with our analyis, we must find the exact value of the circulation prescribed by the Kutta condition. Since we start from the cylinder, our goal is to impose stagnation at the point $B = (\xi_B, \eta_B) = (-b, 0)$, which is then mapped into the trailing edge. This point can also be written in adapted polar coordinates, as: $B = (r_B,\, \theta_B) = (R, \pi + \alpha + \beta)$. By recalling the formulas for velocity components in a circular cylinder, we get:

$$0 = u_r = +U\left(1 - \frac{R^2}{R^2}\right) cos\theta_B = U\,0\,cos\theta_B$$

$$0 = u_\theta = -U\left(1 + \frac{R^2}{R^2}\right) sin\theta_B - \frac{\Gamma}{2\pi R} = -2U sin\theta_b - \frac{\Gamma}{2\pi R}$$

The first equation is trivially satisfied, while the second one leads to a specific value for the circulation:

$$\Gamma = 4\pi R U sin(\alpha + \beta)$$

Since we're imposing a negative velocity $U < 0$, the circulation is also negative, which - in our unconventional construction - corresponds to anticlockwise circulation, in accordance to what we said before.

4.4 Streamlines and Equipotential lines

We are now ready to begin with our analysis. The first thing we want to compute are as usual the velocity potential and the stream function, that can be obtained as the real and imaginary part of the complex potential $w_a(z)$. As mentioned before, the complex potential of the airfoil can be obtained by composing the complex potential of the circular cylinder with the inverse Joukowski transform, that is, by transforming the stream function and the velocity potential we've already computed for the cylinder:

$$w_a(z) = w_c(\zeta(z)) = \phi_c(\zeta(z)) + i\,\psi_c(\zeta(z))$$

One possibility is to perform all explicit computations, by inverting the Joukowski transform and substituting the result in the known formula for the complex potential $w_c(\zeta)$, isolating at last the real and imaginary part. This procedure, however, is quite heavy to perform.

An alternative way is to work directly on the implementation, starting from the last formula we mentioned and exploiting successive grid mapping to represent the composition of functions. We follow this second approach, which will be now explained in detail, with reference to the figures below.

We start from the ζ-plane, where the cylinder will be placed, and we define a mesh, that is, a grid of points, labelled with $j = 1, \ldots, N$ natural index and associated to their cartesian coordinates (ξ_j, η_j). The first goal is to represent in this space the streamlines and equipotential lines of the circular cylinder, which are the level sets of the known polar functions:

$$\phi(r,\theta) = U\left(r + \frac{R^2}{r}\right) cos(\theta) - \frac{\Gamma}{2\pi}\theta \qquad \psi(r,\theta) = U\left(r - \frac{R^2}{r}\right) sin(\theta) + \frac{\Gamma}{2\pi} ln\left(\frac{z}{R}\right)$$

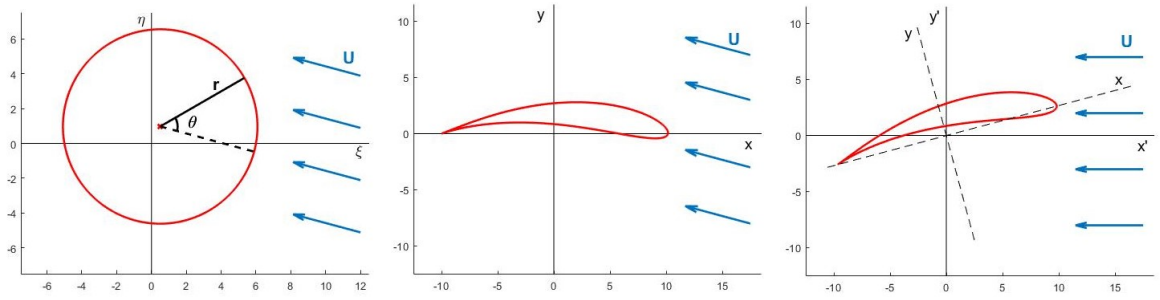

(a) ζ-plane (b) z-plane (c) Final rotation

Figure 12: Mapping grids

They are functions of the adapted polar coordinates (r, θ), defined with origin in the center of the circle and with zero angular coordinate in correspondence of the direction of the fluid coming from infinity. To plot them in the ζ-plane, we must compose these functions with the change of coordinates $(\xi, \eta) \to (r, \theta)$, mapping the cartesian coordinates into the adapted polar coordinates:

$$\begin{cases} \phi(\xi,\eta) = \phi\big(r(\xi,\eta),\, \theta(\xi,\eta)\big) \\ \psi(\xi,\eta) = \psi\big(r(\xi,\eta),\, \theta(\xi,\eta)\big) \end{cases} \qquad \text{with:} \qquad \begin{cases} r(\xi,\eta) = \sqrt{(\xi-\xi_c)^2 + (\eta-\eta_c)^2} \\ \theta(\xi,\eta) = atan\left(\frac{\eta-\eta_c}{\xi-\xi_c}\right) + \alpha \end{cases}$$

where (ξ_c, η_c) are the coordinates for center of the circle and α is the angle of attack.

To implement this composition, we start from the (ξ, η) coordinates associated to each point of the grid and we compute the corresponding adapted polar coordinates (r, θ) using the change of coordinate we've just written. Then, for each point of the grid, we use the polar coordinates to compute the values of $\phi(r, \theta)$ and $\psi(r, \theta)$ using the known formulas we mentioned above. Thus, for each point j of the grid, we know the value of the stream function and of the velocity potential, that can be plotted in correspondence with the (ξ_j, η_j) coordinates in the ζ-plane.

In this way, we performed a composition of functions simply by mapping the original cartesian grid into a new polar grid. The next step consists in repeating the same procedure to compose the functions of interest $\phi(\xi, \eta)$ and $\psi(\xi, \eta)$ with the inverse of the Joukowski transform: $(x, y) \to (\xi, \eta)$.

Since we're dealing with grid mapping instead of analytical composition, there is no need to compute explicitly the inverse of the transformation. We simply start from the mesh we defined in the ζ-plane, we run over the points j and, for each point, we compute the new coordinates (x_j, y_j) applying the direct Joukowski transform to the old coordinates (ξ_j, η_j). We recall that the Joukowski transform acts as follows:

$$x + i\,y \quad = z \quad = \zeta + \frac{b^2}{\zeta} \quad = \xi + i\,\eta + b^2\,\frac{\xi - i\,\eta}{\xi^2 + \eta^2}$$

that is:

$$\begin{cases} x(\xi,\eta) = \xi + \frac{b^2\xi}{\xi^2+\eta^2} \\ y(\xi,\eta) = \eta - \frac{b^2\eta}{\xi^2+\eta^2} \end{cases}$$

In this way, we associate to each j point of the original grid the corresponding $(x_j,\, y_j)$ coordinates on the z-plane.

At this point, the composition of functions $\phi(\xi, \eta)$ and $\psi(\xi, \eta)$ with the inverse Joukowski transform is simply realized by plotting - for each point j of the original grid - the values ϕ_j and ψ_j in correspondence with the (x_j, y_j) coordinates in the z-plane.

With this procedure, we are able to plot the streamlines and equipotential lines in the z-plane, where the airfoil is placed. At this point, the airfoil is horizontal, and the fluid is moving from infinity towards the body with an angle $-\alpha$ with respect to the x axis. It is therefore sufficient to perform a last rotation of the grid to have the desired plot, with the airfoil tilted of an angle α and with the fluid at infinity moving along the x axis.

Finally, we're able to plot the streamlines and equipotential lines around the Joukowski airfoil, as shown in the following figures for three different values of the angle of attack α.

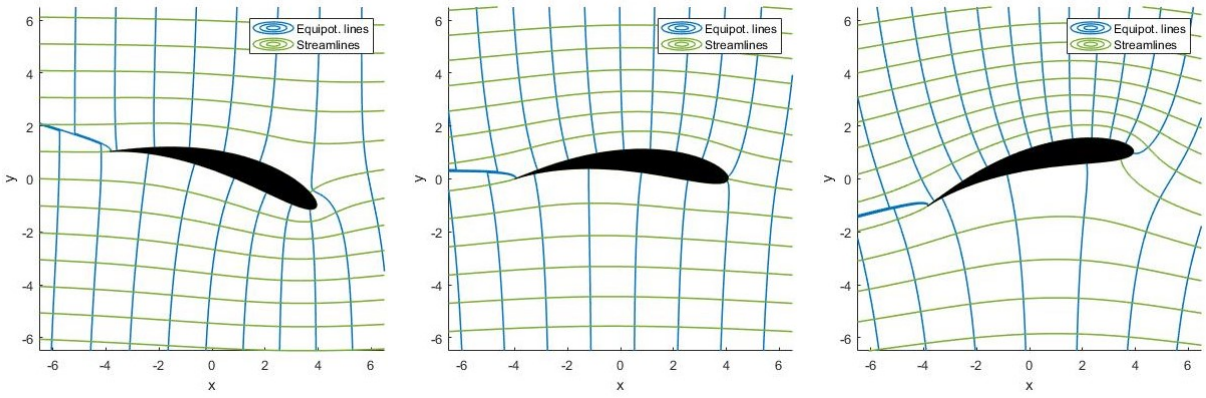

(a) $\alpha = -\frac{\pi}{12}$ (b) $\alpha = 0$ (c) $\alpha = \frac{\pi}{12}$

Figure 13: Streamlines and Equipotential Lines

We observe that in all graphs the streamlines are following the airfoil profile, while equipotential lines are always normal to them. When the angle α is equal to zero, the streamlines are thicker above the body and more spaced below it. This will result in different intensities of the velocity field in the two regions. This effect is more and more evident as the angle α increases, while it is reduced and then progressively inverted when α becomes negative, with a thickening in the lower region and an increased spacing in the upper region. Focusing our attention on the edges, we notice that streamlines are always tangent to the trailing edge, independently of the value of the angle α. This agrees with the intuitive observation we made when presenting the Kutta condition for the circulation. On the other side, the corresponding streamline intersects the leading edge in a different point depending on α, as we naturally expect from the definition of the angle of attack.

4.5 Streaklines

We may now focus on the streaklines, as we did for the cylinder. Since we're studying a stationary flow, the streaklines coincide with the streamlines, and can therefore be treated in the same way, composing the original functions we had for the cylinder with the inverse Joukowski transform through successive grid mapping.

We plot the results for three different values of the angle α.

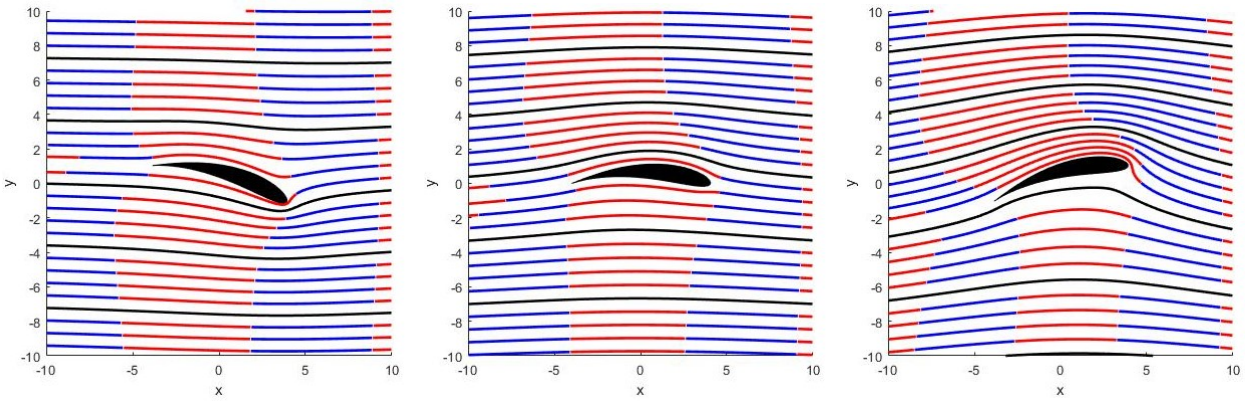

(a) $\alpha = -\frac{\pi}{12}$ (b) $\alpha = 0$ (c) $\alpha = \frac{\pi}{12}$

Figure 14: Streaklines

The pattern of the streaklines coincides with that of the streamlines, as expected. The colors of the blocks allow to get clearer information on the velocity of the particles, which - being the flow stationary - will coincide with the information we get in studying the velocity field.

More in detail, starting from the case $\alpha = 0$, we observe that the length of the blocks is smaller below the cylinder, suggesting slower particles, while is it bigger above the cylinder, where the particles will be faster. This effect becomes more evident as α increases, while it is inverted as α grows negative, with colored blocks which are longer below and shorter above.

4.6 Velocity

We're now interested in computing the velocity field for the airfoil. Following the standard procedure, the two components of the velocity can be obtained by differentiating the complex potential w_a, which can be written as a function of the complex potential w_c of the cylinder, composed with the Joukowski transform. It is therefore sufficient to apply the chain rule, as follows:

$$u_a - i\,v_a = \frac{\partial w_a(z)}{\partial z} = \frac{\partial w_c(\zeta(z))}{\partial z} = \frac{\partial w_c}{\partial \zeta}\cdot\frac{\partial \zeta}{\partial z} = (u_c - i\,v_c)\frac{\partial \zeta}{\partial z}$$

$$\frac{\partial \zeta}{\partial z} = \left(\frac{\partial z}{\partial \zeta}\right)^{-1} = \left(1 - \frac{b^2}{\zeta^2}\right)^{-1} = \frac{\zeta^2}{\zeta^2 - b^2}$$

where $\zeta = \xi + i\,\eta$. By multiplying and dividing for the complex conjugate of the denominator, we can split this quantity in its real and imaginary part:

$$\frac{\partial \zeta}{\partial z} = \frac{(\xi^2-\eta^2)(\xi^2-\eta^2-b^2)+4\xi^2\eta^2}{(\xi^2-\eta^2-b^2)^2+4\xi^2\eta^2} + i\,\frac{(-2\xi\eta b^2)}{(\xi^2-\eta^2-b^2)^2+4\xi^2\eta^2} =: A + i\,B$$

By substituting this into the initial expression for the complex velocity, we get:

$$\begin{cases} u_a = u_c\,A + v_c\,B \\ v_a = v_c\,A - u_c\,B \end{cases}$$

The implementation is therefore straightforward, once we know the velocity components for the circular cylinder. We plot the results for three different angles.

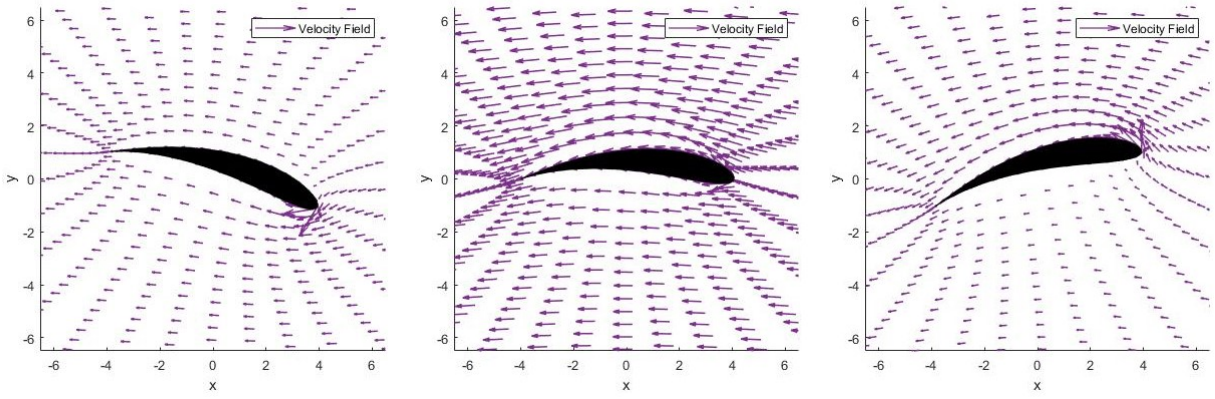

(a) $\alpha = -\frac{\pi}{12}$ (b) $\alpha = 0$ (c) $\alpha = \frac{\pi}{12}$

Figure 15: Velocity Field

We notice that in all graphs the velocity field follows the body profile. When the angle α is zero, the velocity above the airfoil is more intense than the velocity below it, due to the asymmetry of the body. This effect is more marked when the angle α increases, and in this second situation we also observe a strong intensification of the field in correspondence with the leading edge, where the fluid is transported upwards. The behavior is inverted when the angle α grows more and more negative. In this case the difference in speed above and below the cylinder is progressively smoothed, while the intensification of the field in correspondence with the trailing edge is now pointing downwards.

All these observations will have a clear connection with the behavior of the pressure field and with the formation of the forces on the surface of the body.

4.7 Pressure

In order to find the pressure (or, in our case, the normalized pressure $\frac{p-p_\infty}{\rho U^2}$) we can apply the same procedure we used for the circular cylinder, that is, once we have the velocity components (u, v), we apply the Bernoulli theorem:

$$p_\infty + \rho\frac{U^2}{2} = p + \rho\frac{u^2+v^2}{2} \qquad \Leftrightarrow \qquad \frac{p-p_\infty}{\rho U^2} = \frac{1}{2}\left(1 - \frac{u^2+v^2}{U^2}\right)$$

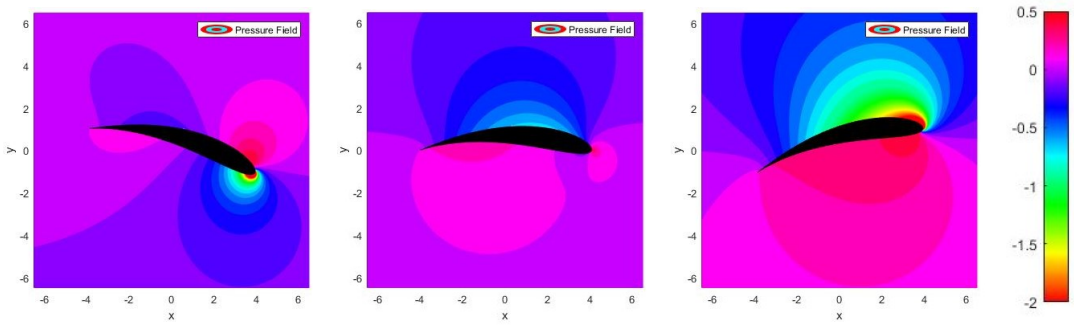

(a) $\alpha = -\frac{\pi}{12}$ (b) $\alpha = 0$ (c) $\alpha = \frac{\pi}{12}$

Figure 16: Pressure Field

The implementation is therefore quite easy once the velocity field is known. We plot the results for the usual three values of the angle α.

By observing the graph for $\alpha = 0$ we notice that the pressure is positive below the airfoil (pink regions), where the velocity is lower, while it is negative above it (blue regions), where the velocity is higher. When we increase the angle α, the behavior is analogous to the one we had for the velocity field: in the lower region, the pressure becomes more and more positive, while in the higher region it becomes more and more negative. In correspondence of the leading edge we observe the same intensification we noticed before, with a negative peak for the pressure. On the contrary, when the angle α grows more and more negative, the region above the airfoil begins to attain positive pressure values, while negative values are attained below the body. Even in this case, we can observe a peak of negative pressure in correspondence with the leading edge.

4.8 Forces

The last part of our analysis consists in describing the elemental forces acting on the surface of the airfoil. They can be computed as in the circular cylinder case, starting from the formula:

$$\vec{F} = -p\hat{n}\, ds$$

In this case the elemental arc length can be approximated by the euclidean distance between two subsequent points on the surface:

$$ds = \sqrt{(x_{i+1} - x_i)^2 + (y_{i+1} - y_i)^2}$$

As for the outer unit normal, we can compute it with good approximation by considering the same two subsequent points on the surface and by rotating the second one (e.g. (x_{i+1}, y_{i+1})) around the first one (e.g. (x_i, y_i)) of an anticlockwise direction:

$$\begin{bmatrix} x_{rot} \\ y_{rot} \end{bmatrix} = \begin{bmatrix} cos\varphi & -sin\varphi \\ sin\varphi & cos\varphi \end{bmatrix} \begin{bmatrix} x_{i+1} - x_i \\ y_{i+1} - y_i \end{bmatrix} + \begin{bmatrix} x_i \\ y_i \end{bmatrix} \qquad = \begin{bmatrix} 0 & -1 \\ 1 & 0 \end{bmatrix} \begin{bmatrix} x_{i+1} - x_i \\ y_{i+1} - y_i \end{bmatrix} + \begin{bmatrix} x_i \\ y_i \end{bmatrix}$$

From this, we can compute the outer normal as:

$$\begin{cases} n_x = x_{rot} - x_i = -(y_{i+1} - y_i) \\ n_y = y_{rot} - y_i = +(x_{i+1} - x_i) \end{cases}$$

and then we normalize it to make it unitary.

With this setting, it is sufficient to know the value of the pressure at the surface to find the forces acting on it, so the implementation is quite natural. We plot the results as the angle α varies, running over the same three values.

Again, the results we obtain for the forces are strictly related to the ones we found for pressure and velocity.

When the angle α is zero, the forces on the upper face of the airfoil are pointing outward, in agreement with the negative values attained by the pressure, while on the lower face, where the pressure is positive, the forces are pointing inward. It is immediate to deduce that the total force acting on the body has a positive y component, resulting in a lift.

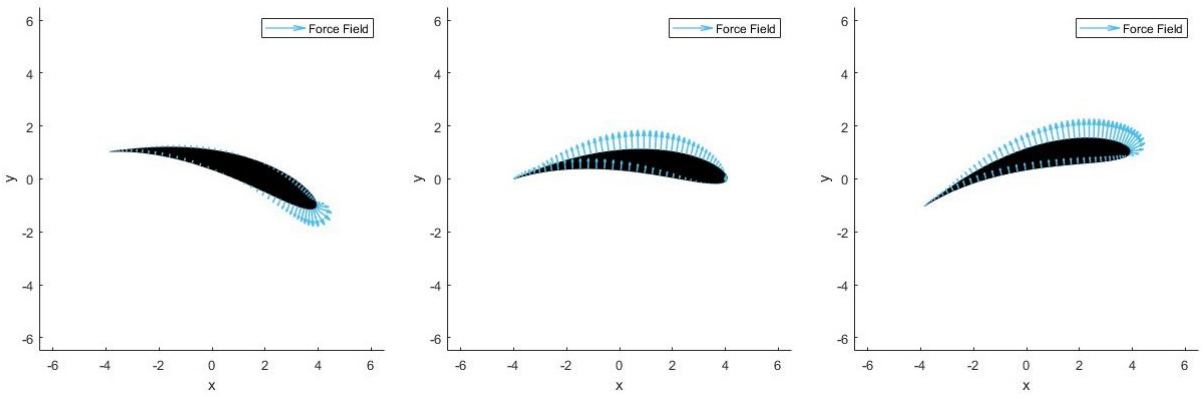

(a) $\alpha = -\frac{\pi}{12}$ (b) $\alpha = 0$ (c) $\alpha = \frac{\pi}{12}$

Figure 17: Forces on surface

When the angle α is increased, this phenomenon is more and more marked, and should result in and higher lift. This, however, is not always true: sooner or later, the gradient of pressure between the negative peak at the edge and the points downstream will be so large that the boundary layer will detach, causing a sudden drop in the lift and therefore the so called "stall" condition.

Finally, when the angle α is negative, we observe the same inverted behavior we noticed before: the intensity of the forces is lowered in both faces, as the pressure is varying from positive to negative and vice versa. The forces on the leading edge present again a peak of intensity, but this time they're pointing downwards.

We might be interested in computing the total force acting on the airfoil. In the following figures, we perform the vector addition of all the elemental forces we derived above, using the head-to-tail method (light blue line). The resulting total force (blue arrow) is clearly vertical, meaning there's only lift force and no drag. We notice that as the effective angle of attack $\alpha + \beta$ is zero - meaning there is no circulation - then the total lift is equal to zero, in accordance with the Kutta-Joukowski Lift Theorem.

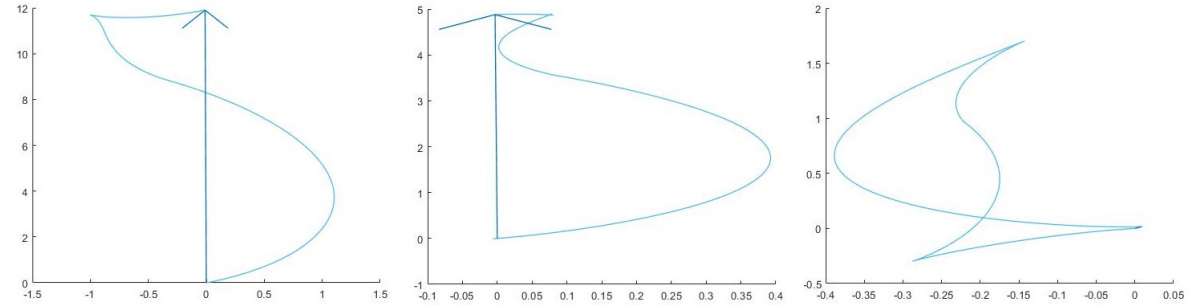

(a) $\alpha = \frac{\pi}{12}$ (b) $\alpha = 0$ (c) $\alpha = -\beta$

Figure 18: Lift force

References

[1] Batchelor G.K. (2002), *An introduction to Fluid Dynamics*, Cambridge University Press, Cambridge.

[2] Colombini M., *Irrotational Plane Flows of an Inviscid Fluid*, http://www.diam.unige.it/ irro/, University of Genoa.

[3] Kundu P.K., Cohen I.M. (2002, second edition), *Fluid Mechanics*, Academic Press, San Diego (California, USA).

[4] Milne-Thompson L.M. (1962, fourth edition), *Theoretical Hydrodynamics*, Macmillan & Co LTD, London.

[5] Olver P.J. (2020, paper), *Complex Analysis and Conformal Mapping*, University of Minnesota.